

Research Article

# Measurement of conversion factor into mean glandular dose in mammography using OSL dosimeters

Yasuki Asada <sup>1,\*</sup> , Honoka Inagaki <sup>2</sup>, Kaito Iwase <sup>2</sup>, Mio Taniguchi <sup>2</sup>, Yuya Nagake <sup>2</sup>, Miuna Hayashi <sup>2</sup><sup>1</sup> Department of Medical Physics, Clinical Collaboration Unit, Faculty of Radiological Technology, School of Medical Sciences, Fujita Health University, Japan<sup>2</sup> Master's Course, Major in Health Sciences, Graduate School of Health Sciences, Fujita Health University, Japan

\*Correspondence: Yasuki Asada (asada@fujita-hu.ac.jp)

**Abstract: Background:** Currently, the DRL quantity in mammography are evaluated in terms of mean glandular dose (MGD). Since the MGD cannot be measured directly, it can be obtained by calculation using the equation ( $D=K \cdot g \cdot c \cdot s$ ). In previous studies, the conversion factor  $g$  was calculated by Monte Carlo simulation and is not reported from actual measurements. In this study, we focused on the  $g$ -factor, which is a conversion factor to the MGD at 50% glandularity, and attempted to measure it using a nanoDot dosimeter to see if it can be used in mammography. **Methods:** The nanoDot dosimeters were inserted in a PMMA phantom at depths ranging from 0 cm to 6 cm in 1 cm increments, and measurements were made in three HVLs of 0.3 mmAl, 0.35 mmAl, and 0.4 mmAl HVL. The  $g$ -factor was calculated from the nanoDot dosimeter values using a conversion equation. **Results and Discussion:** The measured  $g$ -factors for all the HVLs were in close agreement with those of Dance et al. The values of the previous studies did not include the backscatter factor, which may have underestimated the MGD. The difference was smaller for the 0.4 mm Al. Compared to the other HVLs, the 0.4 mm Al was measured without a compression plate, which may have been influenced by the presence or absence of a compression plate. **Conclusion:** The nanoDot dosimeters were used to calculate  $g$ -factors. The results agreed with those of previous studies within uncertainty. This indicates that nanoDot dosimeters can be used in the mammography field.

**Keywords:** G-Factor, Mammography, Mean Glandular Dose, OSL Dosimeter, Backscatter Factor, Diagnostic Reference Level

## How to cite this paper:

Asada, Y., Inagaki, H., Iwase, K., Taniguchi, M., Nagake, Y., & Hayashi, M. (2022). Measurement of conversion factor into mean glandular dose in mammography using OSL dosimeters. *Open Journal of Medical Sciences*, 2(1), 9–16. Retrieved from <https://www.scipublications.com/journal/index.php/ojms/article/view/432>

Received: September 8, 2022

Accepted: October 27, 2022

Published: October 29, 2022



Copyright:© 2022 by the authors. Submitted for possible open access publication under the terms and conditions of the Creative Commons Attribution (CC BY) license (<http://creativecommons.org/licenses/by/4.0/>).

## 1. Introduction

The International Commission on Radiological Protection (ICRP) recommends that Diagnostic Reference Levels (DRLs) should be used in the process of optimization in radiation diagnosis [1]. The first DRLs in Japan were published in June 2015 [2] and revised in 2020 [3]. DRL quantity in mammography are evaluated in terms of mean glandular dose (MGD). Since the MGD cannot be measured directly, it can be obtained by calculation. Equation (1) shows the equation [4-6] of Dance et al for obtaining the MGD.

$$D = K \cdot g \cdot c \cdot s \quad (1)$$

where  $D$  is the MGD [mGy],  $K$  is the incident air kerma [mGy],  $g$  is the conversion factor to the MGD with 50% glandularity,  $c$  is the factor correct for the difference in composition of typical breasts from 50% glandularity, and  $s$  is the factor for the target and filter combination.

Besides Dance *et al.*, the conversion factors to MGD were also reported by Wu *et al.* [7, 8]. It was also reported by Sobol *et al.* [9] that the conversion factor could be calculated using VBA (Visual Basic for Applications™) code. Software to estimate the MGD using this code has also been developed [10]. In recent years, however, the use of characteristic X-rays using Mo targets has been decreasing due to the widespread of digital equipment and improved image processing technology and is being replaced by W targets [11]. Therefore, the conversion factors of Wu *et al.* using Mo and Rh targets have become difficult to deal with. On the other hand, the equation of Dance *et al.* using the *s*-factor, which is the factor due to the combination of target and filter, has become popular. The conversion factor *g* in Equation. (1) is a value obtained from Monte Carlo simulations and is not reported from actual measurements. For actual measurements, ionization chamber dosimeters are often used, but it is difficult to insert an ionization chamber dosimeter into a PMMA phantom because of the physical size of the chamber itself. However, the nanoDot dosimeter, an optically stimulated luminescence (OSL) dosimeter that has been reported to be able to measure entrance surface dose (ESD) with an accuracy of about 15% [12] and backscatter factor [13], is very small ( $10 \times 10 \times 2 \text{ mm}^3$ ), has a wide measurement range (10  $\mu\text{Gy}$  to 10 Gy) and energy range (5 keV to 20 MeV) [14], and has high detection sensitivity and almost no fading effects [15]. The nanoDot dosimeter, which is used in the diagnostic field, could also be used in the mammography field because of its features such as the ability to take multiple readings without erasing the element information.

In this study, we focused on the *g*-factor, which is a conversion factor to the MGD at 50% glandularity, and attempted to measure it using a nanoDot dosimeter to see if the nanoDot dosimeter can be used in mammography field.

## 2. Materials and Methods

### 2.1. Instruments

In this study, the mammography system was a Sepio (Shimadzu Manufacturing corporation, Kyoto, Japan), the OSL dosimeter was a nanoDot dosimeter (Nagase Landauer Ltd, Ibaraki, Japan), the OSL dosimeter measurement system was a microStar (Nagase Landauer Ltd, Ibaraki, Japan), the phantom was a semicircular PMMA phantom ( $\Phi 16 \text{ cm}$ , 1 cm thick). Measurement of half value layer (HVL) was a Radcal Accu Gold+ (Radical Corporation, California, USA), and the calibration of the nanoDot dosimeter was used an ionization chamber dosimeter of a model 9015 (10X5-6M) (Radical Corporation, California, USA).

The semi-circular PMMA phantom used in this study simulates the shape of a breast, and was processed so that nine nanoDot dosimeters could be inserted (Figure 1).

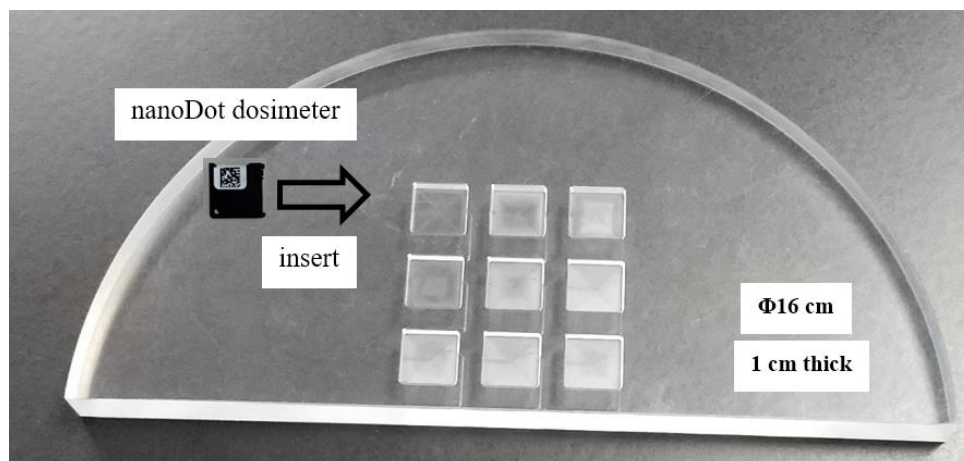


**Figure 1.** PMMA phantom processed for nanoDot dosimeter insertion.

## 2.2. Determination of exposure conditions

The HVL used in this study were 0.30 mm Al, 0.35 mm Al, and 0.40 mm Al. The target was Mo and the filter was Mo. To determine the exposure conditions that would result in the above HVLs, the HVLs were measured using an X-ray analyzer. The exposure conditions obtained from the results are shown in Table 1. For the films shown in Table 1, two polystyrene sheets were attached to the radiation inlet to adjust the HVL to 0.40 mmAl.

Table 1. Exposure conditions.

HVL [mmAl]	Tube voltage[kV]	mA second[mAs]	Target/Filter	Compressed plate	SSD [cm]
0.30	23	100	Mo/Mo	+	53
0.35	30	50		+	
0.40	32	50		(2 films)	

HVL: half value layer, SSD : Source surface distance, + : with, - : without

## 2.3. Calculation of g-factor

The arrangement of nanoDot dosimeters in the dosimetry is shown in Figure 2. 9 nanoDot dosimeters were inserted in a 1 cm thick PMMA phantom. The nanoDot dosimeters were inserted in the phantom and measured under the exposure conditions shown in Table 1, varying the depth every 1 cm from 0 cm to 6 cm. The nanoDot dosimeter was multiplied by the calibration constant of each element and air kerma, read five times each, and the average of the three readings, excluding the maximum and minimum values, was used as the measured value. The average value was calculated from the nine readings obtained and normalized by the value at 0 cm depth to obtain a relative value.

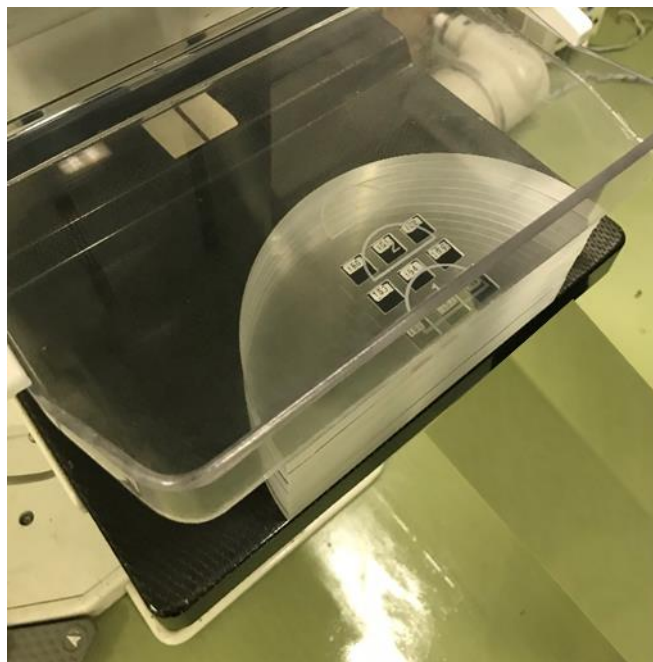


Figure 2. Geometry for dosimetry.

From the obtained relative values, a PDD CURVE (percentage depth dose curve) was created and an approximate equation was obtained. Equation (2) shows the formula for calculating  $X_g$  [16,17].

$$X_g = \frac{1}{\tau - 1} \int_{0.5}^{\tau - 0.5} x_g z dz \quad (2)$$

where  $X_g$  is the ratio of the dose at depth  $z$  to the dose at the incident surface in the breast model [16] at thickness  $\tau$ ,  $x_g(z)$  is the ratio of the dose at depth  $z$  to the dose at the incident surface, and  $\tau$  is the PMMA thickness.

From the obtained  $X_g$ , the  $g$ -factor (conversion factor) in the actual measurement was calculated. Equation (3) shows the formula for calculating the  $g$ -factor in the actual measurement.

$$\text{Conversion factor} = 0.00090 \cdot 1000 \cdot X_g / 100 \quad (3)$$

where 0.00090 is the value to convert 0.79 mrad / R of the  $f$ -factor of the breast to mGy / mGy [16,17].

Note that all nanoDot dosimeters used were calibrated for use as air kerma by each tube voltage (HVL) under the exposure conditions in Table 1. For the calibration method, 10 nanoDot dosimeters were simultaneously exposed to the ionization chamber dosimeter. Three exposures were performed at each tube voltage (0.3, 0.35, and 0.4 mmAl in HVL), and the average value was used as the calibration constant for each element.

### 3. Results

The PDD curve for a HVL of 0.3 mmAl is shown in Figure 3. The dose decreased exponentially with depth. Approximate equations and coefficients of determination for each HVL are also shown. The coefficients of determination of the approximate equations for each HVL are above 0.99, indicating that the equations are reflected. Table 2 shows the  $g$ -factors for each PMMA thickness at the HVL= 0.30 mm Al, 0.35 mm Al, and 0.40 mm Al in Figures 4, 5, and 6, respectively.

**Table 2. Backscatter factor for mammography.**

HVL [mmAl]	Backscatter Factor
0.30	1.07
0.35	1.08
0.40	1.09
0.45	1.10

HVL: half value layer

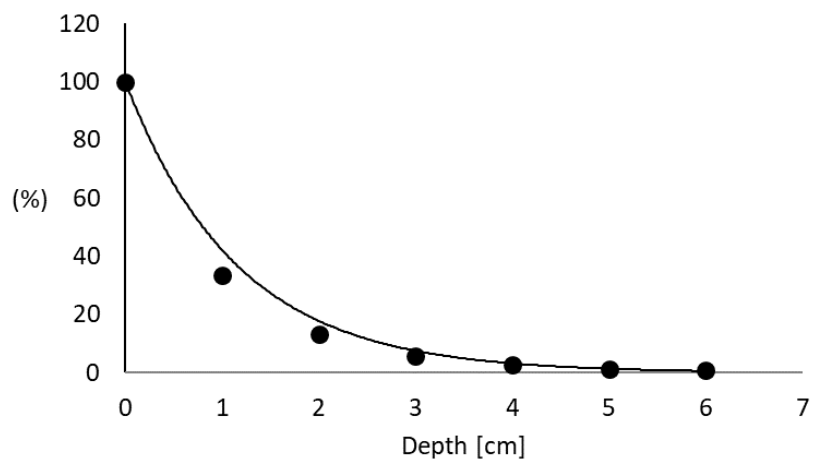


**Figure 3.** PDD curve (HVL=0.3 mmAl).

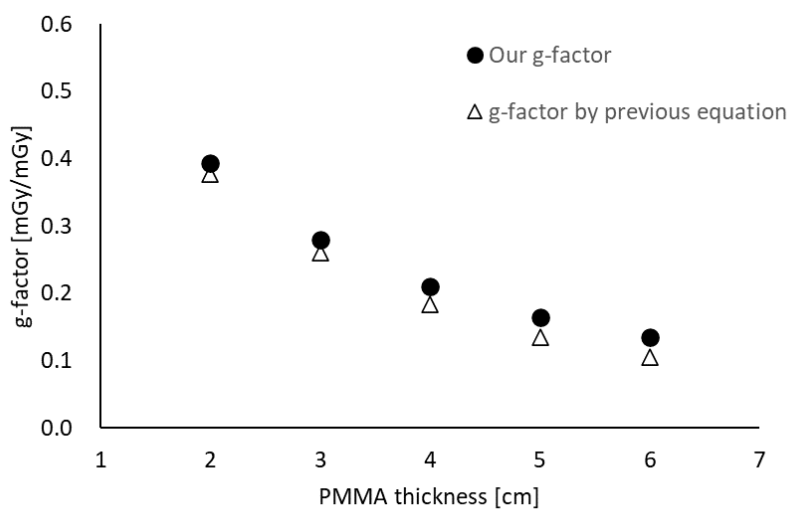


**Figure 4.** g-factor (HVL:0.3 mmAl).

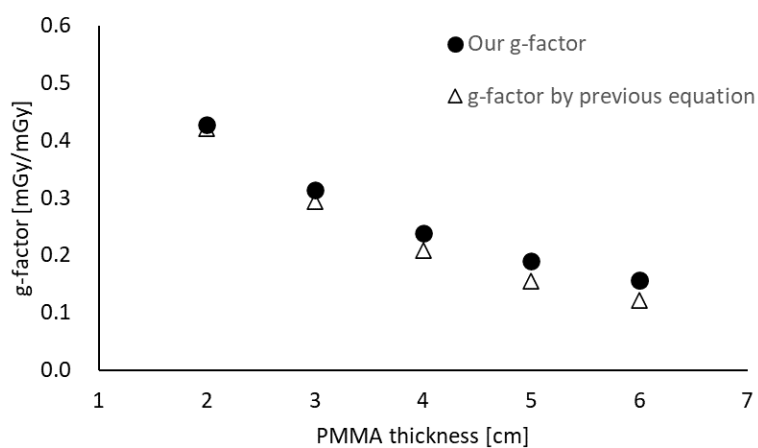


**Figure 5.** g-factor (HVL:0.35 mmAl).

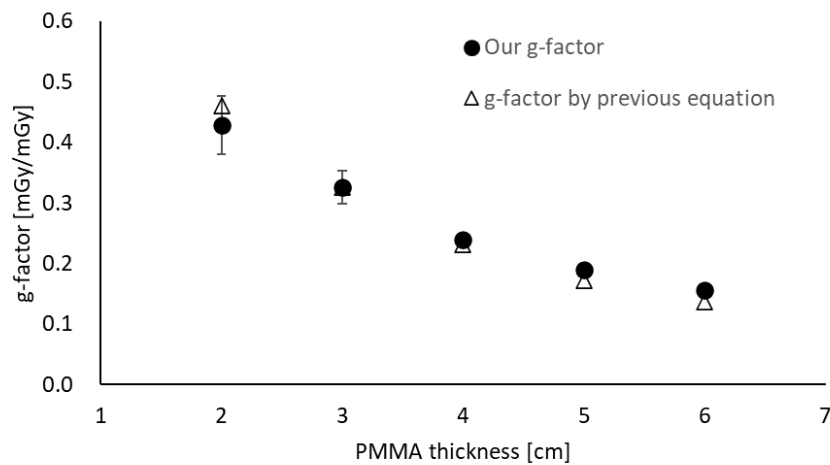


**Figure 6.**  $g$ -factor (HVL:0.4 mmAl).

For all HVLs, the measured  $g$ -factors are in close agreement with those of Dance et al. However, as the PMMA thickness increased, the measured  $g$ -factor tended to be larger than that of Dance et al. However, the difference was smaller at 0.40 mm Al.

#### 4. Discussion

In Japan, DRL was first introduced in 2015 [2] and revised in 2020 [3], with DRL quantities and DRL values published for CT, general radiography, mammography, dental radiography, interventional radiography (IVR), diagnostic fluoroscopy, and nuclear medicine. The DRL quantity for mammography is the MGD. In the evaluation, the average dose to the breast is evaluated because of the higher risk of the mammary gland, rather than the dose at the incident surface, which is the maximum dose as in general radiography. For this purpose, a factor to convert into the MGD is needed. Currently, the  $g$ -factor of Dance et al. is used [4-6].

MGD conversion factors other than those of Dance et al. include a backscattering-factor or multiply by an appropriate backscatter factor [18], as reported by Stanton et al. However, the  $g$ -factor of Dance et al. does not take this backscatter factor into account. For the calculation of MGD, the incident dose in air without backscatter is measured using a Sharrow-type ionization chamber dosimeter and multiplied by the MGD conversion factor [19]. This is true for DRL measurements as well, but only for instrumental quality control, and the backscatter factor is considered necessary in consideration of actual patient exposure. Therefore, we focused on the nanoDot dosimeter, which can be used without any problem in terms of direction dependence, except for scattering in the 90° direction [20], and has an uncertainty of about 10 % [21]. There is also a report of measuring backscatter factor using the nanoDot dosimeter [13], so we used it in this study.

The results show that for thicker PMMA phantoms, the measured  $g$ -factor is larger than the existing  $g$ -factor of Dance et al. In the measured values, the dose ratio decreased exponentially with depth, suggesting that the difference between the nanoDot dosimeter, which includes a certain amount of backscatter factor, and the existing  $g$ -factor, which does not account for backscatter, increased with depth. Table 3 shows the backscatter factors for mammography recommended by European protocols in the HVLs used in this study. It can be seen that there is a backscatter of up to 10% at 0.45 mm Al in the HVL [22]. It should also be noted that the results indicate that thicker phantom thicknesses may lead to underestimation of the MGD. The fact that the difference between the present study and existing values was smaller for the 0.4 mmAl HVL than for the other HVLs may be due to the presence or absence of a compression plate, since the 0.4 mmAl was measured

without a compression plate to make the beam quality concerned, while the compression plate was attached for the other HVLs.

**Table 3. PDD Curve.**

HVL [mmAl]	Target/Filter	approximate equation	R <sup>2</sup>
0.30	Mo/Mo	$y = 100e^{-0.086x}$	0.9913
0.35		$y = 100e^{-0.077x}$	0.9939
0.40		$y = 100e^{-0.077x}$	0.9961

HVL: half value layer

## 5. Conclusion

The measured g-factors values using the nanoDot dosimeter tended to be larger as the PMMA thickness increased, which was attributed to the effect of backscatter factor. However, the measured results of the nanoDot dosimeter were in close agreement with the g-factor of Dance *et al.* even after taking uncertainties into account. Therefore, it can be said that nanoDot dosimeters used in the diagnostic field can also be used in the mammography field.

## References

- [1] International Commission on Radiological Protection: Radiological protection and safety in medicine. ICRP Publication 73. Annals of the ICRP. 1996; 26(2).
- [2] Japan DRLs 2015, "Diagnostic Reference Levels Based on Latest Surveys in Japan - Japan DRLs", <http://www.radher.jp/JRIME/report/DRLhoukokusyo.pdf>. (Accessed 2022.6.29).
- [3] Japan DRLs 2020, "Diagnostic Reference Levels Based on Latest Surveys in Japan - Japan DRLs", <http://www.radher.jp/JRIME/report/DRLhoukokusyoEng.pdf> (Accessed 2022.6.29).
- [4] D R Dance, Monte Carlo calculation of conversion factors for the estimation of mean glandular breast dose, *Pys. Med. Biol.*, 1990, 35, 9, 1211-1219.
- [5] D R Dance, C L Skinner, K C Young, J R Beckett and C J Kotre, Additional factors for the estimation of mean glandular breast dose using mammography dosimetry protocol *Pys. Med. Biol.*, 2000, 45, 3225-3240.
- [6] N. Perry, M. Broeders, C. de Wolf, S. Törnberg, R. Holland, L. von Karsa, E Puthaar, European guidelines for quality assurance in breast cancer screening and diagnosis Fourth edition Luxembourg, 2006, European Communities.
- [7] X Wu, G T Barnes, D M Tucker, Spectral dependence of glandular tissue dose in screen-film mammography, *Radiology*, 1991, 179, 143-148.
- [8] X Wu, E L Gingold, G T Barnes, D M Tucker, Normalized average glandular dose in molybdenum target-rhodium filter and rhodium target-rhodium filter mammography, *Radiology*, 1994, 193, 83-89.
- [9] W T Sobol, X Wu, Parametrization of mammography normalized average glandular dose tables, *Med Phys.*, 1997, 24, 4, 547-54.
- [10] Y Asada, K Nishi, T Kamei, S Fujii and S Suzuki, Software for Estimation of Patient Dose in Mammography, *Jpn. J. Radiol. Technol.*, 2001, 57, 12, 1511-1518. (in Japanese)
- [11] Y Asada, Y Kondo, M Kobayashi, K Kobayashi, T Ichikawa and Y Matsunaga, Proposed diagnostic reference levels for general radiography and mammography in Japan, *J. Radiol. Prot.*, 2020, 40, 867-876.
- [12] K Takegami, H Hayashi, H Okino, N Kimoto, I Maehata, Y Kanazawa, T Okazaki, I Kobayashi, Practical calibration curve of small-type optically stimulated luminescence (OSL) dosimeter for evaluation of entrance skin dose in the diagnostic x-ray region, *Radiol Phys Technol.*, 2015, 8, 286-94.
- [13] A Arimoto, Y Asada, Investigation of backscatter factor in medical radiography using anthropomorphic phantom by optically stimulated luminescence dosimeter, *Biomed Phys Eng Express*, 2021, 7, 6, DOI: 10.1088/2057-1976/ac21ac.
- [14] Nagase Landauer, dosimetry system "microStar" <https://www.nagase-landauer.co.jp/download/pdf/microStar.pdf> (Accessed 2022.6.29). (in Japanese)
- [15] Paulina Elzbieta Wesolowska, Andrew Cole, Tania Santos, Tomislav Bokulic, Pavel Kazantsev and Joanna Izewska, Characterization of three solid state dosimetry systems for use in high energy photon dosimetry audits in radiotherapy, *Radiation Measurements*, 2017, 106, 556-562.

- 
- [16] Leonard Stanton, Theodore Villafana, John L. Day, Davis A. Lightfoot, Dosage Evaluation in Mammography, *Radiology*, 1984, 150, 577-584.
- [17] G Richard Hammerstein, Daniel W Miller, David R White, Mary Ellen Masterson, Helen Q Woodard and John S Laughlin, Absorbed Radiation dose in Mammography, *Radiology*, 1979, 130, 485-491.
- [18] R Kramer, G Drexler, N Petoussi-Henss, M Zankl, D Regulla and W Panzer, Measurements of diagnostic x-ray backscatter by novel ion chamber method, *Med. Phys.*, 1982, 9, 1, 121-130.
- [19] Japanese Society of Radiological Technology, Standard measurement methods of the absorbed dose in the diagnosis X-rays region, Ohmsha, Tokyo, Japan, 2017, 26-27. (in Japanese)
- [20] Rani M Al-Senana, Mustapha R Hatab, Characteristics of an OSLD in the diagnostic energy range, *Med Phys.*, 2011, 38, 7, 4396-4405.
- [21] Landauer, nanoDot™ Dosimeter Patient Monitoring Solutions. 50749 NanoDot FDA.pdf (landauer.com). (Access 2020.12.11).
- [22] R Kramer, G Drexler, N Petoussi-Henss, M Zankl, D Regulla and W Panzer, Backscatter factors for mammography calculated with Monte Carlo methods, *Phys. Med. Biol.*, 2001, 46, 771-781.